The PsbU Subunit of Photosystem II Stabilizes Energy Transfer and Primary Photochemistry in the Phycobilisome−Photosystem II Assembly of *Synechocystis* sp. PCC 6803†

John Veerman,‡ Fiona K. Bentley,§ Julian J. Eaton-Rye,§ Conrad W. Mullineaux,|| Sergei Vasil'ev,‡ and Doug Bruce*,‡

Department of Biological Sciences, Brock University, St. Catharines, Ontario L2S 3A1, Canada, Department of Biochemistry, University of Otago, P.O. Box 56, Dunedin, New Zealand, and School of Biological Sciences, Queen Mary, University of London, Mile End Road, London E1 4NS, U.K.

Received June 14, 2005; Revised Manuscript Received October 28, 2005

ABSTRACT: The PsbU subunit of photosystem II (PSII) is one of three extrinsic polypeptides associated with stabilizing the oxygen evolving machinery of photosynthesis in cyanobacteria. We investigated the influence of PsbU on excitation energy transfer and primary photochemistry by spectroscopic analysis of a PsbU-less (or ΔPsbU) mutant. The absence of PsbU was found to have multiple effects on the excited state dynamics of the phycobilisome and PSII. ΔPsbU cells exhibited decreased variable fluorescence when excited with light absorbed primarily by allophycocyanin but not when excited with light absorbed primarily by chlorophyll *a*. Fluorescence emission spectra at 77 K showed evidence for impaired energy transfer from the allophycocyanin terminal phycobilisome emitters to PSII. Picosecond fluorescence decay kinetics revealed changes in both allophycocyanin and PSII associated decay components. These changes were consistent with a decrease in the coupling of phycobilisomes to PSII and an increase in the number of closed PSII reaction centers in the dark-adapted ΔPsbU mutant. Our results are consistent with the assumption that PsbU stabilizes both energy transfer and electron transport in the PBS/PSII assembly.

Photosystem II (PSII)[1] is the site of water splitting and oxygen evolution during oxygenic photosynthesis (*1*). This pigment−protein complex consists of at least 19 proteins, with ∼16 being integral membrane subunits, and the complex contains ∼36 chlorophyll (Chl) molecules (*2*). Two Chl *a*-binding core antenna subunits known as CP43 and CP47 (*3*, *4*) serve to absorb incident light and funnel the energy into the reaction center of the complex. The reaction center is composed of the D1 and D2 protein subunits, which contain a Chl dimer known as P680, that serves as the primary donor for electron transport (*1*, *2*). Oxidation of P680 results in the successive oxidation of the inorganic core of the oxygen-evolving complex (OEC). This incorporates a manganese cluster containing Ca^{2+} and Cl^- cofactors (*2*, *5*) that exists in five oxidation or S-states which undergo a cyclic pathway of univalent oxidation steps from states S_o to S_4, returning to S_o after O_2 release (*6*). The OEC is located on the lumenal side of the thylakoid membrane, and in cyanobacteria the surrounding environment additionally contains the extrinsic PsbO, PsbU, and PsbV (or cytochrome *c*-550) protein subunits (*7*).

The efficiency of primary photochemistry is largely dependent on the ability of the organism to absorb photons and direct the energy into the PSII reaction center so that charge separation and plastoquinone reduction can take place (*1*). This is achieved by transferring energy through peripheral antenna complexes to the core antenna pigment proteins. In cyanobacteria, the peripheral complex is the phycobilisome (PBS), which serves as antenna to both PSII and photosystem I (PSI). Changes in the distribution of absorbed energy between PSII and PSI are regulated via the light state transition (*8*−*10*).

The mechanism(s) by which the PBS physically binds to the thylakoid membrane and/or photosystems are unclear as are the details of PBS energy coupling to PSII and PSI. An exogenous hydrophobic linker polypeptide consisting of 54 amino acid residues, and referred to as the PB loop, has been implicated in PBS/thylakoid interactions (*9*, *10*). However, there is also evidence that indicates that PSII has a native binding affinity for the PBS, even in the absence of the PB loop (*11*, *12*), and it is possible that the PBS may associate with the membrane through interactions with lipid headgroups (*13*). It has been suggested that the terminal emitter

† This work was supported by grants from the Natural Sciences and Engineering Research Council of Canada to D.B., by a New Zealand Marsden grant (UOO309) to J.J.E.-R., and by grants from the Biotechnology and Biological Sciences Research Council (U.K.) to C.W.M.

* Address correspondence to this author. Telephone: (905) 688-5550 ext 3826. Fax: (905) 688-1855. E-mail: dbruce@ brocku.ca.

‡ Brock University.

§ University of Otago.

|| University of London.

[1] Abbreviations: DCMU, 3-(3,4-dichlorophenyl)-1,1-dimethylurea; DAS, decay-associated spectra; F_o, dark-adapted fluorescence yield when photosystem II traps are open; F_m, dark-adapted fluorescence yield when photosystem II traps are closed; F_v, $F_m - F_o$; FRAP, fluorescence recovery after photobleaching; HEPES, 4-(2-hydroxyethyl)-1-piperazineethanesulfonic acid; OEC, oxygen-evolving complex; PBS, phycobilisome(s); PCC, Pasteur Culture Collection; PCR, polymerase chain reaction; PSI, photosystem I; PSII, photosystem II; TES, 2-[[tris(hydroxymethyl)methyl]amino]-1-ethanesulfonic acid.

10.1021/bi051137a CCC: $30.25
Published on Web 12/01/2005

or the PBS ApcE anchor polypeptide is required for PBS assembly and PBS/PSII energy coupling (*14*). Fluorescence recovery after photobleaching (FRAP) measurements support a transient binding of PBS to PSII, as they show diffusion rates for the PBS to be much higher than for PSII (*10*, *13*). Despite the lack of agreement on the precise mechanism of binding and energy coupling, it is clear that changes in orientation or distance of the PBS from PSII would greatly affect energy transfer efficiency (*8*).

The 12 kDa PsbU protein, encoded by *psbU*, is thought to impart structural stability to the OEC and to shield the manganese complex from cellular reductants. Inactivation of the *psbU* gene in *Synechococcus* sp. PCC 7002 demonstrated that PsbU stabilized oxygen evolution at elevated temperatures and was also required for the acquisition of cellular thermotolerance (*15*, *16*). Similar results were obtained with *Synechocystis* sp. PCC 6803 although the requirement of PsbU was less stringent in this strain (*17*). In addition, in vivo, the removal of PsbU also resulted in reducing oxygen evolution to ~80% of the wild-type rate, and photoautotrophic growth was slowed in the absence of either Ca^{2+} or Cl^- and abolished under $CaCl_2$-limiting conditions (*17*−*19*). Moreover, thermoluminescence measurements have demonstrated that the S_2 state of the OEC is modified in ΔPsbU cells where the recombination reactions are shifted to higher temperatures for both the Q- and B-bands (*18*).

The importance of PsbU for optimal rates of oxygen evolution was also observed in vitro where full reconstitution of PSII activity required the rebinding of PsbU to isolated PSII complexes from *Thermosynechococcus vulcanus* and removal of PsbU in ΔPsbO cells prevented photoautotrophic growth in a ΔPsbO:ΔPsbU strain of *Synechocystis* sp. PCC 6803 (*20*, *21*). Despite the importance of PsbU for PSII activity the number of PSII centers assembled in ΔPsbU cells was found to be similar to wild type when assayed using 3-(3,4-dichlorophenyl)-1,1-dimethylurea (DCMU) replaceable [^{14}C]atrazine binding to detect assembled photosystems (*22*). Unexpectedly, assays of PSII abundance using variable Chl *a* fluorescence yield measurements indicated that fluorescence was quenched in the ΔPsbU strain (*22*). The present study was undertaken to determine the origin of the quenched variable fluorescence and ascertain the effect of PsbU removal on energy transfer and primary photochemistry in PSII. To this end the *psbU* gene in *Synechocystis* sp. PCC 6803 was interrupted to produce a ΔPsbU strain which was then characterized by room temperature, low temperature, and picosecond time-resolved fluorescence spectroscopy. Our results indicate that both energy transfer from the PBS to PSII and primary photochemical processes within PSII were altered in the ΔPsbU mutant.

MATERIALS AND METHODS

Growth of Synechocystis sp. PCC 6803 Strains. Cultures were maintained on BG-11 plates containing 5 mM glucose and 20 μM atrazine, and when required, chloramphenicol was present at a concentration of 15 μg/mL in both solid and liquid BG-11 media. The solid media were supplemented with 10 mM TES−NaOH (pH 8.2) and 0.3% sodium thiosulfate (*23*), and liquid cultures were grown photoautotrophically unless otherwise noted. Cells were grown under a continuous illumination of 30 μE m^{-2} s^{-1}, and the temperature in the growth chamber was 30 °C. The *Synechocystis* sp. PCC 6803 strain used in this study was the glucose-tolerant strain from Williams (*24*), and this is referred to throughout as wild type.

Construction of a Synechocystis sp. PCC 6803 Strain Lacking PsbU. The open reading frame sll1194, encoding the PsbU protein, was obtained by PCR using the forward primer 5′-CCCAAAATCGGATCCGTCGGCATAATTTTC-3′ and the reverse primer 5′-AAAGGGTACGCAATG-GAATTCGGTTAGCAG-3′. The underlined bases correspond to introduced *Bam*HI and *Eco*RI sites, respectively, that were incorporated into the primer design and used to clone the PCR product into pUC19 (New England BioLabs). The cloned *psbU* gene was interrupted at a unique intragenic *Swa*I site by a chloramphenicol resistance cassette derived from pBR325 (*25*, *26*) and then used to transform *Synechocystis* sp. PCC 6803 according to established protocols (*23*, *24*). Complete segregation for the introduced antibiotic resistance cassette was verified by PCR using the forward and reverse primers described above.

Photoinactivation and Oxygen Evolution Assays. For these measurements cells were grown in BG-11 containing 5 mM glucose before being harvested for the experiments. Following the removal of glucose, cells, maintained at 30 °C and at a Chl *a* concentration of 10 μg/mL, were inactivated by 2.0 mE m^{-2} s^{-2} of white light provided by a Kodak Ektalite 1000 slide projector. Oxygen evolution was measured with a Clark-type electrode (Hansatech) at 30 °C in BG-11 containing 25 mM HEPES−NaOH, pH 7.5. Saturating actinic light (2 mE m^{-2} s^{-1}) was provided by an FLS1 light source (Hansatech) passed through a Melis Griot OG 590 sharp cutoff red glass filter. The electron acceptors were 3.0 mM $K_3Fe(CN)_6$ and 0.6 mM 2,5-dimethyl-*p*-benzoquinone. When added, lincomycin was at 250 μg/mL.

Room Temperature Fluorescence. Cell cultures were placed in a 1 cm path glass cuvette at a volume of ~3 mL and dark adapted to state 2 (*27*), and measurements were made with a PAM fluorometer (model Pam 101; H. Walz, Effeltrich, Germany). The minimal Chl *a* fluorescence yield, F_o, was determined by exposing dark-adapted cells to a low intensity modulated measuring light of either 655 or 440 nm (*28*). To obtain the variable Chl *a* fluorescence yield, F_v, saturating white light pulses of 600 ms duration were used to close the PSII reaction centers and determine the maximum fluorescence yield, F_m, from which F_v was calculated as $F_m - F_o$.

77 K Fluorescence Emission Spectra. Cells were harvested during exponential growth phase, and the ΔPsbU mutant and wild-type samples were adjusted to equal absorbance at 435 nm as determined with an Aminco DW-2 absorbance spectrometer equipped with a light scattering correcting frosted glass between the sample and photomultiplier tube. Samples were dark adapted to state 2 and then transferred to glass tubes that were ~5 mm in radius and 10 cm in length with one end sealed. Tubes were placed in a dewar filled with liquid N_2 and positioned so that the glass tube could be manually turned about its lengthwise axis while retaining its position and orientation. Fluorescence emission spectra were collected using an EG&G 1461 diode array detector (E.G. & G., Salem, MA) as described previously (*29*). To account for position-sensitive variation in fluorescence yield

from the frozen samples, each sample tube was rotated incrementally and measured a total of 16 times to generate one averaged emission spectra. Three independent repeats of this procedure were used to generate the final emission spectrum for each sample.

Fluorescence Decay Kinetics. Fluorescence decay kinetics were measured with dark-adapted whole cell cultures at a Chl *a* concentration of 10 μg/mL using the single photon timing apparatus previously described (*30*−*32*). Both the 407 and 650 nm picosecond pulsed diode lasers (Picoquant, Berlin, Germany) used for excitation were operated at 10 MHz. For each measurement a 200 mL sample was circulated at a flow rate of ∼4 mL s^{-1}. The detector was a Hamamatsu R3809 microchannel plate (Hamamatsu). Decay data were collected in 4096 channels over 50 ns with a Becker & Hickl SPC-630 single photon timing card (Berlin, Germany) in a Pentium PC. Decay data were collected at F_o from dark-adapted samples and F_m from preilluminated samples in the presence of DCMU as described in ref *32*.

Global Lifetime Analysis. Global lifetime analyses of fluorescence decays at multiple emission wavelengths were done as described previously (*32*). The detection wavelength ranges were 640−730 nm for 650 nm excitation and 660−730 nm for 407 nm excitation, taken at 10 nm increments. All programs used for data manipulation and global analysis were written by Sergei Vassiliev.

Chlorophyll and Phycocyanin Determination. Chlorophyll concentrations were determined from methanol extracts by the method of MacKinney (*33*). Phycocyanin concentrations were determined from whole cell absorption by the method of Myers et al. (*34*).

RESULTS

Construction and Physiology of the ΔPsbU Mutant. The strategy to construct the ΔPsbU mutant used in this report is shown in Figure 1A. Also shown is the result of a PCR using primers specific for the *psbU* gene and confirming full segregation of the inactivated *psbU* carrying a 2.0 kb chloramphenicol resistance cassette in the ΔPsbU strain. The rates of oxygen evolution for the ΔPsbU mutant were found to be ca. 52% of the wild-type rate (Figure 1B). In addition, the effect of 45 min illumination at 2 mE m^{-2} s^{-1} is shown. In wild-type cells the initial rate of oxygen evolution was reduced by 20% while the ΔPsbU strain exhibited only 32% of its initial rate and underwent rapid photoinactivation during the period that the actinic light was on. The susceptibility of the ΔPsbU mutant to high light was investigated in the time course shown in Figure 1C. Rates of oxygen evolution in ΔPsbU cells exposed to 2 mE m^{-2} s^{-1} illumination fell by ca. 50% within 30 min. In contrast, oxygen evolution rates in the wild type initially decline by ca. 25% but then were able to acclimate to the high light conditions. These data suggest that the rate of repair of photodamaged PSII was able to keep up with the rate of inactivation in the wild type but not in the ΔPsbU mutant under these conditions. This interpretation was supported by the addition of lincomycin before the onset of the high light treatment. Under these conditions oxygen evolution in the wild type was reduced by 50% in ca. 80 min, although in the ΔPsbU cells PSII activity declined at a similar rate in the presence or absence of lincomycin. However, without the protein synthesis inhibitor, PSII activity of the ΔPsbU mutant remained at ca. 30% of the initial level before exposure to high light, whereas PSII activity was completely abolished in the presence of lincomycin. We also found that photoinactivated ΔPsbU cells recovered oxygen-evolving activity to the level observed before exposure to 2 mE m^{-2} s^{-1} illumination following a further incubation at 0.07 mE m^{-2} s^{-1} over 2 h and that this recovery was completely prevented by the presence of lincomycin (data not shown).

The results obtained in Figure 1 therefore confirm that the ΔPsbU cells created for this study represented a homoplasmic line and that oxygen-evolving activity was impaired in agreement with earlier studies (*17*, *22*). These cells were therefore used to evaluate the anomalously low estimates of PSII abundance measured in ΔPsbU cells using Chl *a* variable fluorescence yield measurements as previously reported (*22*).

Room Temperature Fluorescence. Steady-state room temperature variable fluorescence (F_v) was measured using a PAM fluorometer. Figure 2 clearly indicates that variable fluorescence (F_v/F_m) of the ΔPsbU mutant was decreased when compared to the wild type when using a 655 nm measuring light (preferentially exciting allophycocyanin). The data in Figure 2 were not normalized, and wild-type and ΔPsbU mutant samples were at equal Chl concentrations. This revealed that much of the decrease observed in F_v/F_m arose from a large increase in F_o in the ΔPsbU mutant relative to wild-type cells. Interestingly, the F_v/F_m of the ΔPsbU mutant was not smaller than that of the wild type when variable fluorescence was determined with 440 nm measuring light (preferentially exciting Chl *a*) although both the F_o and F_m levels of the wild type were slightly lower than those of the ΔPsbU strain. Observation of the decreased F_v/F_m in the ΔPsbU mutant was thus dependent on excitation of the phycobilisome. These data suggest that the decreased F_v/F_m in the mutant arises from an increase in phycobilin fluorescence contributing to the F_o yield and not necessarily to an intrinsic change in PSII photochemistry. This was confirmed with room temperature emission spectra at F_o and F_m, shown in Figure 3. For excitation of the PBS at 600 nm the emission spectra of both F_o and F_m in the ΔPsbU mutant and wild type are dominated by phycobilin fluorescence. The data from mutant and wild type are similar; however, the relative contribution of phycobilin to Chl emission is higher in the ΔPsbU mutant. In both wild type and mutant the contribution of Chl to the F_o emission spectra is minimal. The F_o spectra are also characterized by a long-wavelength tail, a characteristic of phycobilin emission, that extends beyond 740 nm.

From the shape of the room temperature emission spectra it is clear that the amplitude of F_v/F_m, determined with a PAM type fluorometer, will depend heavily on the detection wavelength and the excitation wavelength of the instrument. The emission filter used in the standard PAM fluorometer is a long pass (>710 nm) red filter which will unfortunately block the bulk of the Chl *a* variable fluorescence and allow detection of much of the long-wavelength phycobilin emission. This will have the effect of decreasing the apparent F_v/F_m when determined with phycobilisome excitation wavelengths. As the contribution of phycobilin fluorescence relative to Chl fluorescence is higher in the ΔPsbU mutant than in the wild type (Figure 3), the F_v/F_m as measured with

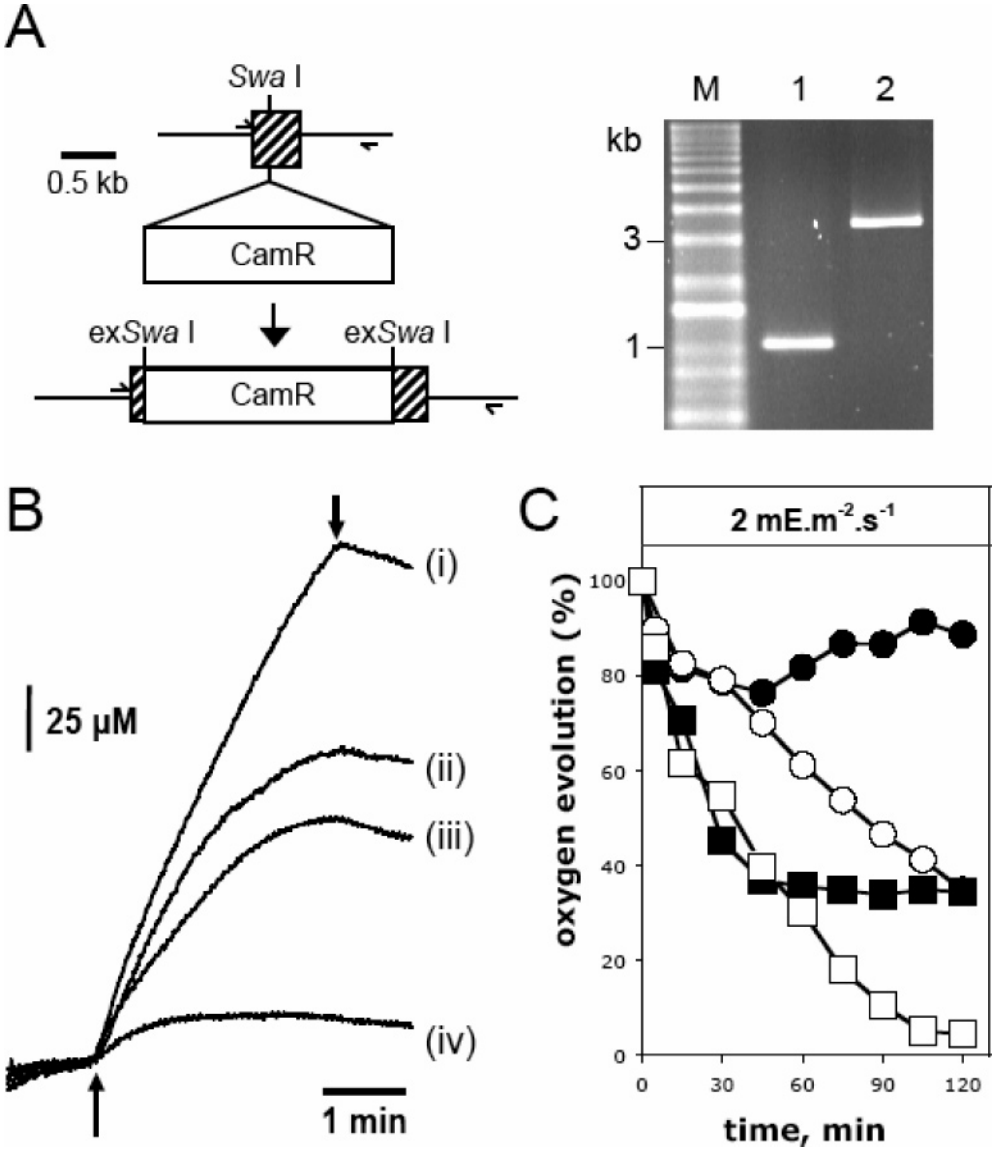

FIGURE 1: Construction of the ΔPsbU mutant. (A) Diagram of the *psbU* region in the *Synechocystis* sp. PCC 6803 genome with or without the insertion of a 2.0 kb chloramphenicol-resistance marker (CamR) inserted at a *SwaI* site 160 bp from the initial base of the start codon. A PCR was run that confirmed complete replacement of *psbU* with the interrupted gene in the ΔPsbU strain. The primers used in the reaction are indicated with arrows. The lanes on the gel are as follows: M, 1 kb Plus DNA ladder, supplied by Invitrogen; 1, PCR product from wild type; 2, PCR product from the ΔPsbU strain. (B) Oxygen evolution traces before and after illumination at 2 mE m^{-2} s^{-1} with white light. Traces: (i) wild type at 0 min, 503 μmol of O_2 (mg of Chl)$^{-1}$ h^{-1}; (ii) wild type after 45 min illumination, 402 μmol of O_2 (mg of Chl)$^{-1}$ h^{-1}; (iii) ΔPsbU at 0 min, 262 μmol of O_2 (mg of Chl)$^{-1}$ h^{-1}; (iv) ΔPsbU after 45 min illumination, 84 μmol of O_2 (mg of Chl)$^{-1}$ h^{-1}. The data in panel B were repeated in three independent experiments with similar results. (C) Time course of photoinactivation of oxygen evolution in wild type (circles) and ΔPsbU (squares). Open symbols contain lincomycin. The results from two independent experiments are shown. The Chl concentration was 10 μg mL^{-1} during exposure to 2 mE m^{-2} s^{-1} of white light and during the oxygen evolution assays in panels B and C.

the PAM appears lower in the mutant cells for excitation at 650 nm. Chlorophyll fluorescence makes a much larger relative contribution to the room temperature emission for Chl *a* excitation (data not shown), and F_v/F_m determinations with the PAM for excitation at 440 nm are not as confounded by phycobilin emission and are thus more similar in mutant and wild-type cells. However, at either excitation wavelength the multiple components contributing to the steady-state PAM fluorescence measurements complicate the interpretation of variable fluorescence and limit the conclusions made possible by simple comparisons of F_v/F_m.

Absorbance spectra of the ΔPsbU mutant and wild-type cells show similar relative contributions from Chl *a* and phycobilin pigments (data not shown). The fluorescence yield of phycobilin pigments is, however, consistently higher in the ΔPsbU mutant than in the wild type when samples are measured at either equal Chl (data not shown) or equal phycocyanin concentrations (Figure 3). This increased phycobilin fluorescence may be characteristic of a partially decoupled PBS.

To investigate energy transfer from the PBS to Chl *a* in the thylakoid membrane, 77 K fluorescence emission spectra were determined (Figure 4). The 77 K fluorescence spectra of the ΔPsbU mutant and wild type were similar when 435 nm light was used to preferentially excite Chl *a* (Figure 4, upper panel). In contrast, excitation of the PBS with 600 nm light revealed large differences between the ΔPsbU mutant and wild type (Figure 4, lower panel). The ΔPsbU

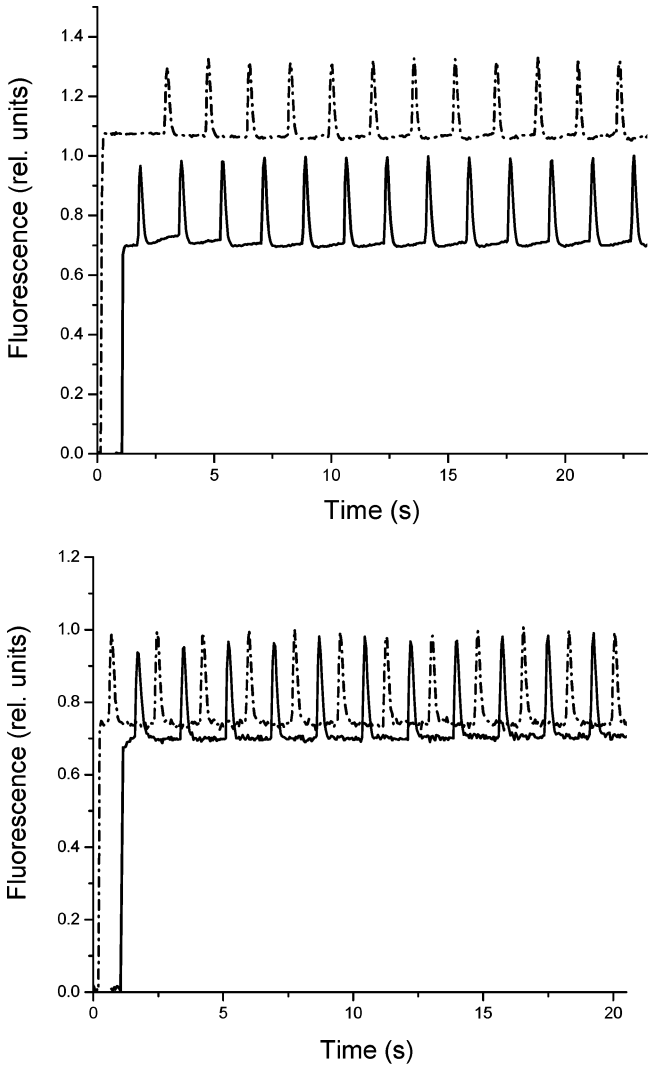

FIGURE 2: Pulse amplitude modulated (PAM) room temperature fluorescence kinetic traces. Upper panel, excitation wavelength 665 nm; lower panel, excitation wavelength 440 nm. Solid traces are for wild type and dashed traces for the ΔPsbU strain. Wild-type and ΔPsbU cells were at equal Chl concentrations. Multiple turnover saturating white light flashes (600 ms duration) were used to determine F_m (spikes on traces). Traces are not normalized. This experiment was repeated five times; a representative trace is shown. Repeated measures of F_o and F_m between individual experiments were within 10%.

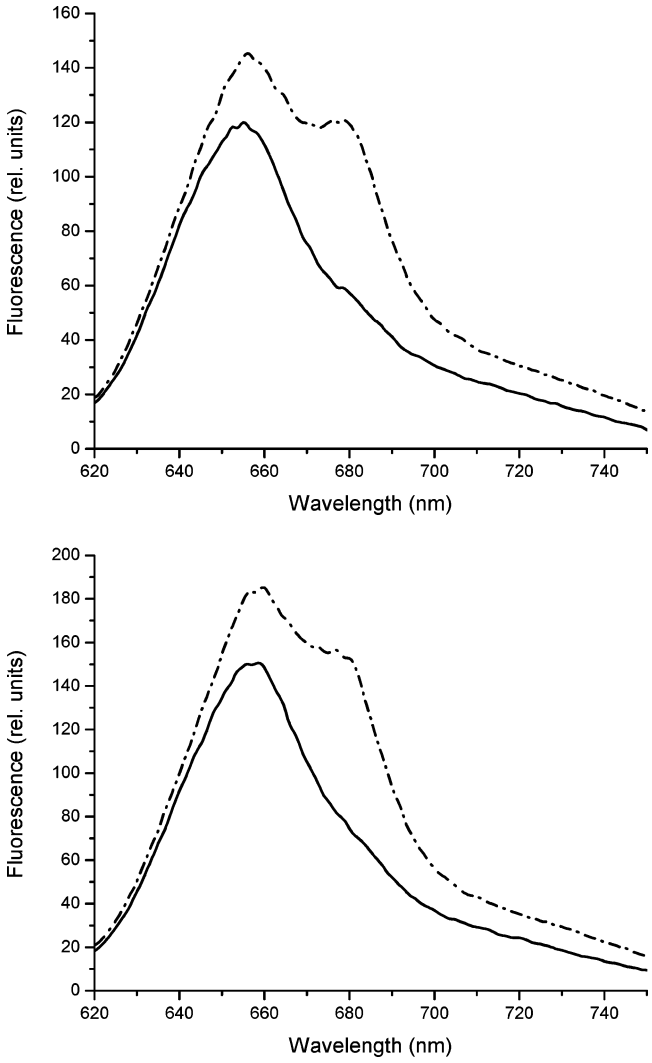

FIGURE 3: Room temperature fluorescence emission spectra. The excitation wavelength was 600 nm. The upper panel is wild type and lower panel is the ΔPsbU strain. All samples were measured at equal phycocyanin concentrations. Solid lines are cells at F_o, and dashed lines are cells at F_m (see text for details).

mutant is characterized by increased emission from allophycocyanin at 665 nm relative to phycocyanin at 650 nm and by a large increase in the 685 nm peak, which has contributions from both PSII Chl *a* and the terminal phycobilin emitters, relative to all other emission peaks. The 695 nm emission peak (red-shifted core antenna Chl in CP47) does not increase with the 685 nm peak, which suggests that the increase observed at 685 nm results mostly from the terminal phycobilin emitters rather than PSII core antenna Chl. The 77 K emission data are thus consistent with a decrease in efficiency of energy transfer from PBS to Chl *a* in the ΔPsbU cells.

Changes in the relative efficiency of energy transfer from the PBS to PSII and to PSI are regulated by the light state transition in cyanobacteria. The increase in emission at 685 nm in the ΔPsbU mutant is somewhat reminiscent of the increases in emission at 685 and 695 nm (PSII Chl *a*) relative to 725 nm (PSI Chl *a*) that are characteristic of the transition to light state 1 in cyanobacteria. To investigate possible connections, we compared state transitions in the wild type and ΔPsbU mutant. As shown in Figure 5 the ΔPsbU cells are state transition competent and undergo transitions of similar magnitude (changes in F_v) to the wild type as assayed by room temperature fluorescence kinetics. Changes in 77 K fluorescence emission spectra typical of light state transitions and of similar magnitude to those observed in the wild type are also observed in the ΔPsbU mutant (data not shown). The increase in emission at 685 nm observed in the 77 K emission spectra of the ΔPsbU mutant relative to the wild type is thus not indicative of cells with an inhibited state transition that are "stuck" in state 1.

Fluorescence Decay Kinetics. Picosecond fluorescence decay kinetics were collected to help to interpret the differences in emission we observed between the wild type and ΔPsbU mutant with steady-state fluorescence spectroscopy. The fluorescence decay kinetics at F_o for the ΔPsbU strain and wild type are shown in Figure 6 for excitation at 407 nm (absorbed by phycocyanin, allophycocyanin, and Chl *a*) and for excitation at 650 nm (absorbed predominantly by

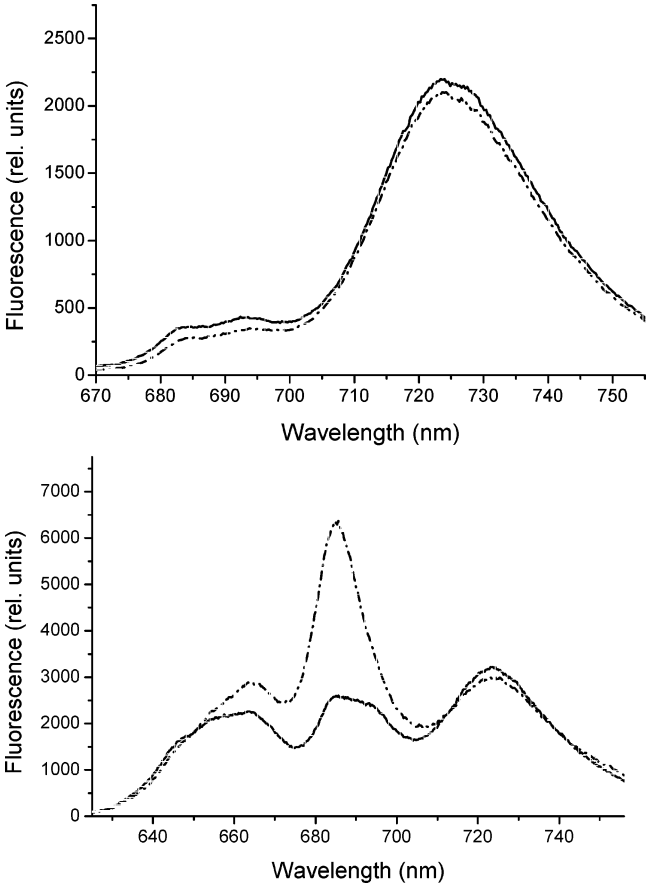

FIGURE 4: 77 K fluorescence emission spectra of wild type and the ΔPsbU strain using dark-adapted cells excited at either 435 nm (upper panel) or 600 nm (lower panel). Solid lines are for wild-type cells, and the dashed lines are for the ΔPsbU strain. Samples were all at equal Chl concentrations. Spectra were collected from three independent experiments; one representative trial is presented. Spectra were not normalized. Repeat measures of peak amplitudes between independent experiments were within 10%.

allophycocyanin). Both excitation wavelengths generated decay kinetics that were slower in the ΔPsbU cells than in the wild type. This suggests that differences between the wild type and mutant may not be restricted to phycobilin emission.

Global Lifetime Analysis. A global fluorescence decay analysis was done to characterize the individual decay components contributing to the altered fluorescence decay kinetics resulting from loss of PsbU. As described previously (*31*), fluorescence decays were collected at a number of emission wavelengths and fit simultaneously to a sum of exponential decay components. Component lifetimes were assumed invariant across emission wavelength, and decay-associated spectra (DAS) were constructed by plotting the yield of each decay component as a function of emission wavelength. This approach facilitates the separation of the many components contributing to steady-state fluorescence emission and offers more insight into the origins of changes in variable fluorescence. To further facilitate the identification of the origin of the decay components, two different excitation wavelengths were used. Excitation pulses at 407 nm were used to excite Chl *a*, phycocyanin, and allophycocyanin to similar extents whereas the 650 nm excitation was used to more selectively excite allophycocyanin.

The DAS from both wild-type and ΔPsbU cells at F_o are shown in Figure 7 for excitation at 650 nm and at 407 nm.

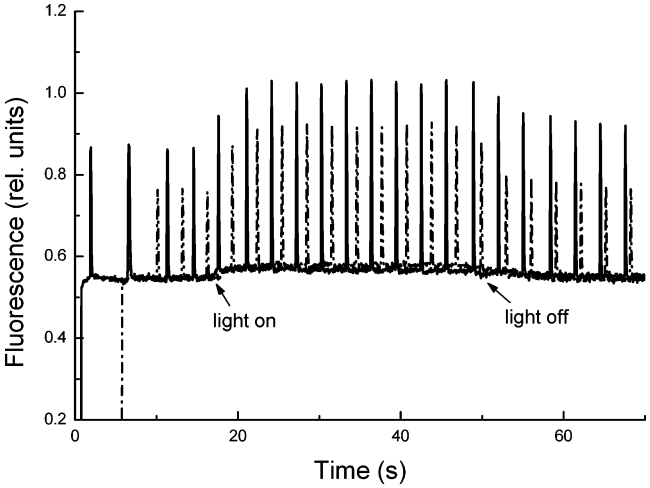

FIGURE 5: Pulse amplitude modulated (PAM) fluorescence kinetic traces for wild type (solid line) and for the ΔPsbU strain (dashed line). The excitation wavelength was 665 nm. F_m was determined with saturating flashes (600 ms) of white light (spikes on traces). Dark-adapted cells (state 2) were exposed to blue light excitation (430 nm excitation, 100 μE m^{-2} s^{-1}) to induce a transition to state 1. The blue light was turned on and off as shown by the arrows underneath the traces. Samples were measured at equal Chl concentrations; the trace for the ΔPsbU strain was displaced vertically downward so that the traces overlapped at the F_o level to facilitate comparison of the blue light induced changes in F_v.

The fastest kinetic component had a lifetime of approximately 40 ps and was observed only for excitation at 407 nm. This component was clearly a mixture of at least two components as it had a negative yield (rise component) at short wavelengths and a positive yield (decay component) at longer wavelengths. The short wavelength negative peak at 660 nm likely reflects a rise component in allophycocyanin emission resulting from energy transfer from phycocyanin to allophycocyanin. The longer wavelength peak at 690 nm with a shoulder at 710 nm is typical of PSI decay. The yield of this component did not change when PSII reaction centers were closed by illumination in the presence of DCMU (Figure 8), which is also consistent with these assignments. A component with a lifetime of approximately 150 ps peaking at 660 nm was observed for 650 nm excitation and 407 nm excitation in both mutant and wild-type cells. This component was by far the major contributor to decay for 650 nm excitation but had a much smaller relative yield for excitation at 407 nm. The yield of this component was independent of PSII trap closure (Figure 8). This and the emission peak at 660 nm clearly localize this component to the PBS. Both phycocyanin and allophycocyanin may contribute to this component at 407 nm excitation, but due to its strong absorption at 650 nm allophycocyanin will dominate the decay at 650 nm excitation. The lifetime of this component may thus reflect excitation energy transfer processes from phycocyanin to allophycocyanin to the terminal long-wavelength phycobilin emitters and also possibly from allophycocyanin to Chl *a*. This component makes very similar contributions to wild-type and ΔPsbU cells under all conditions, suggesting that these kinetic processes are relatively unaffected by the lack of PsbU.

A decay component with a shoulder at 660 nm and a peak at 680 nm having a lifetime in the 300 ps region was seen for excitation at both 407 and 650 nm. Interestingly, the spectral shape of this component was independent of

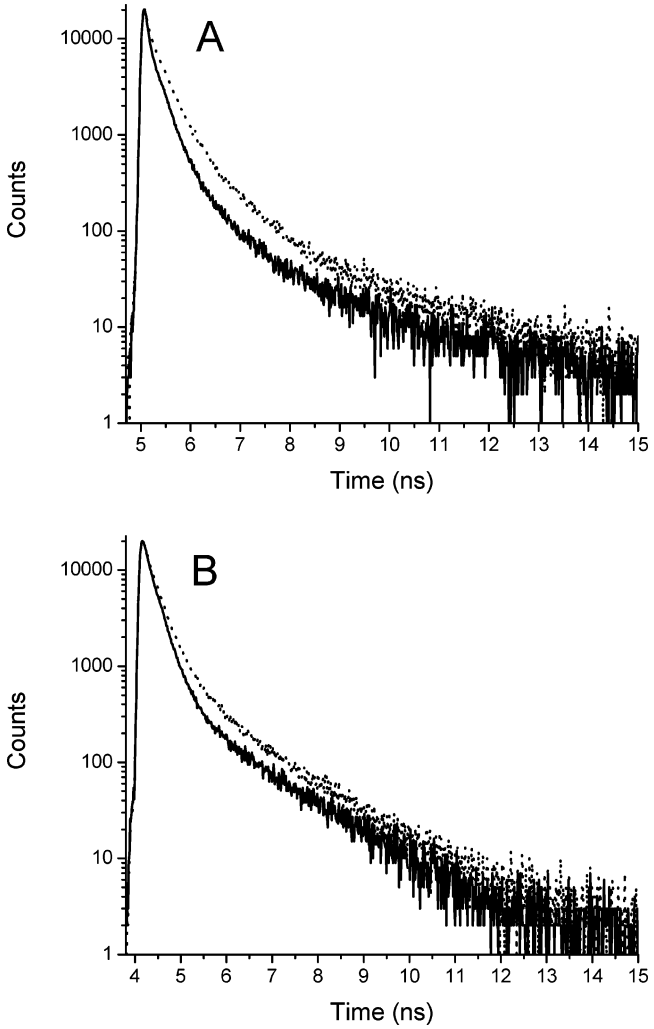

FIGURE 6: Fluorescence decay kinetics of wild type (solid trace) and ΔPsbU strain (dotted trace) for excitation at 407 nm (panel A) and at 650 nm (panel B). The emission wavelength was 680 nm. The traces are for dark-adapted cells at F_o; data were collected to 30000 counts in the peak channel.

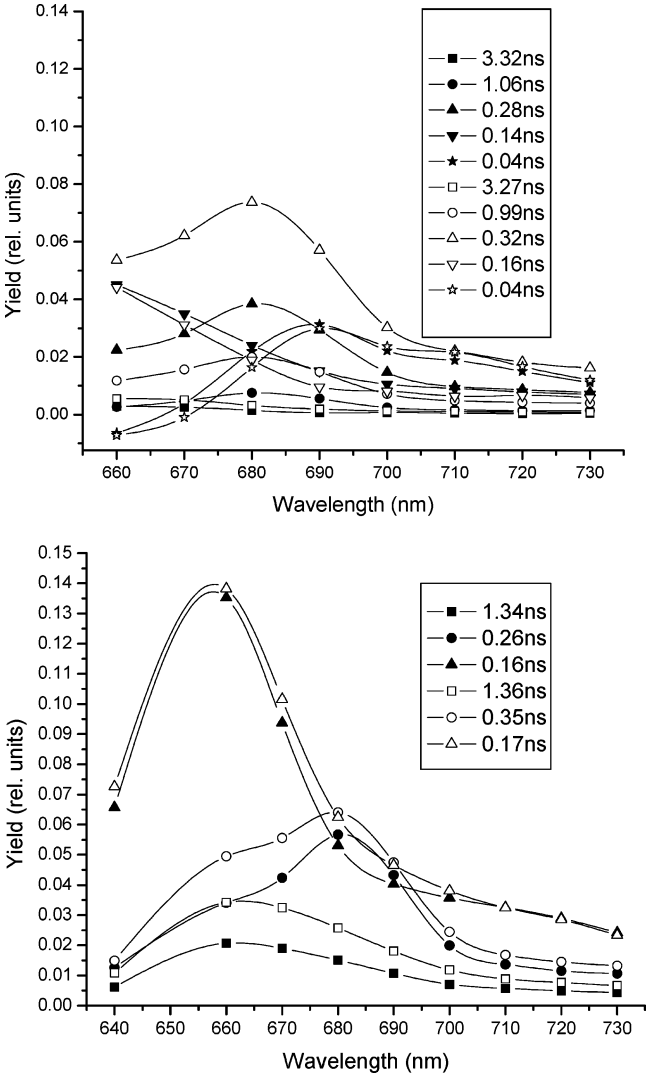

FIGURE 7: Decay-associated spectra (DAS) of globally fitted fluorescence decay kinetics from dark-adapted wild type (filled symbols) and ΔPsbU cells (open symbols) at F_o for excitation at 407 nm (upper panel) and for excitation at 650 nm (lower panel). The fluorescence yields (lifetime × amplitude) of each decay component are plotted versus emission wavelength. Five decay components were required for the global fit of the decay data for 407 nm excitation; the χ^2 value was 1.08 for the mutant and 1.09 for the wild type. Three decay components were required for the global fit of the decay data for 650 nm excitation; the χ^2 value was 1.14 for the mutant and 1.13 for the wild type. Cells were measured at equal Chl concentrations, and overall fluorescence yields (sum of all decay components) were normalized to the steady-state fluorescence emission yields.

excitation wavelength. This component was the largest contributor to the decay for excitation at 407 nm and the second largest for excitation at 650 nm. The yield of this component increased by approximately 30−40% when PSII reaction centers were closed by illumination in the presence of DCMU (Figure 8). At 407 nm excitation the lifetime of this component was almost invariant across samples. In the wild type the lifetime was 280 ps at F_o and 310 ps at F_m and in the mutant 325 ps at F_o and 320 ps at F_m. Interestingly, for 650 nm excitation the lifetime of this component appeared to increase upon trap closure and was also somewhat longer in the mutant than the wild-type cells at both F_o and F_m. Lifetimes in the control were 265 ps at F_o and 320 ps at F_m, and in the mutant they were 350 ps at F_o and 400 ps at F_m. The most striking feature of this component was the much larger contribution it made to the overall decay at F_o in the mutant than in the control at both excitation wavelengths (Figure 7). This was especially apparent at 407 nm, where the yield of this component in the ΔPsbU mutant was twice that of the wild type. For all conditions the relative contribution of the 660 nm emission to the 680 nm emission of this component was larger in the mutant than the wild type. The spectra of this component suggest emission from PBS core components (allophycocyanin and the terminal phycobilin emitters) and PSII Chl *a*. It is interesting that the shape of the 300 ps decay component spectra is the same for excitation at 407 nm (bilin and Chl *a*) and at 650 nm (predominantly allophycocyanin). This could be consistent with an equilibrium population of PBS core components and PSII Chl *a*. Upon trap closure, the spectral shape remains the same, and changes in the amplitude of this component were more dominant than changes in its lifetime. Photosystem II associated decay components in intact cyanobacteria were previously reported to change yield rather than lifetime upon trap closure (*35*). Our 300 ps decay component may have such an origin and arise from Chl *a* and PBS core components that are tightly coupled energetically and whose

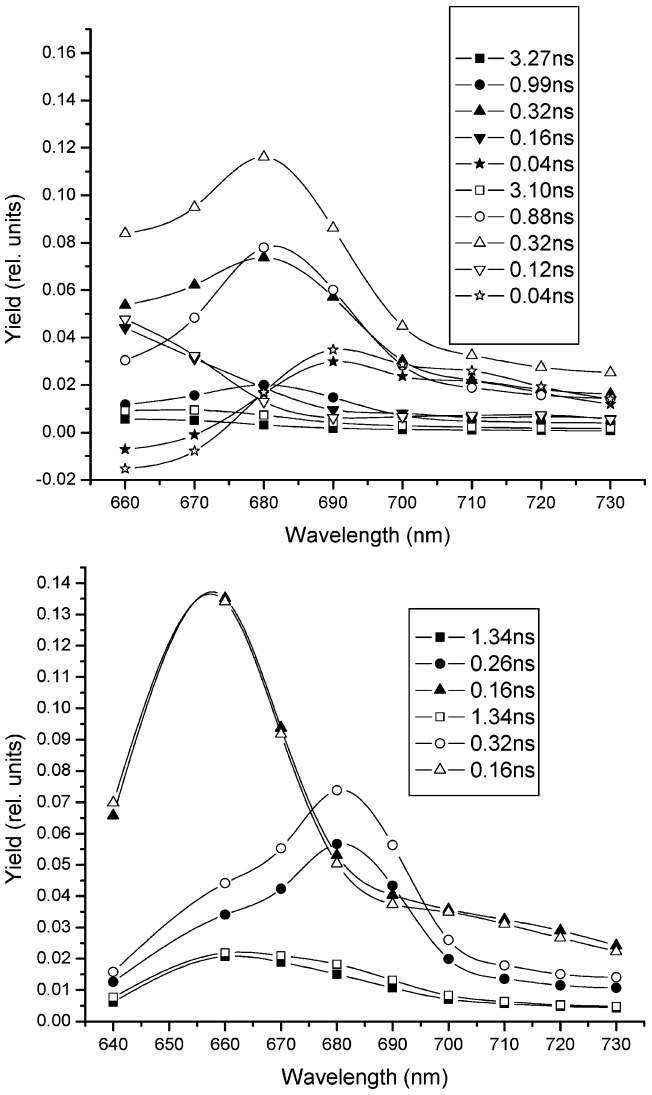

FIGURE 8: Decay-associated spectra (DAS) of globally fitted fluorescence decay kinetics from dark-adapted cells. The fluorescence yields (lifetime × amplitude) of each decay component are plotted versus emission wavelength. The upper panel shows the ΔPsbU strain at F_o (filled symbols) and F_m (open symbols) for excitation at 407 nm. Five decay components were required for the global fit of the decay data for 407 nm excitation; the χ^2 value was 1.08 for the F_o data and 1.14 for the F_m data. The lower panel shows wild-type cells at F_o (filled symbols) and F_m (open symbols) for excitation at 650 nm. Three decay components were required for the global fit of the decay data for 650 nm excitation; the χ^2 value was 1.13 for the F_o data and 1.14 for the F_m data. Cells were measured at equal Chl concentrations, and overall fluorescence yields (sum of all decay components) were normalized to the steady-state fluorescence emission yields.

lifetimes predominantly reflect the processes within PSII. An alternative possibility, especially for the 650 nm excitation of allophycocyanin, is that the component reflects emission from the core of the PBS and the lifetime is related to the relative efficiency of energy transfer to Chl *a* and/or some other quencher.

Two slow decay components with nanosecond lifetimes were distinguished with excitation at 407 nm, the faster one with an approximately 1 ns decay and a clear peak at 680 nm and the slower, a 3.3 ns component peaking at 660 nm. Upon trap closure the yield of the 1 ns component increased greatly in both mutant and wild type (Figure 8 shows the mutant data), identifying its origin in closed PSII reaction centers as described previously (*35*, *36*). The yield of the 3.3 ns component was much smaller and not as sensitive to trap closure. In contrast, at 650 nm excitation a 1.3 ns decay component with a peak at 660 nm and broad shoulder at 680 nm was observed. In both mutant and wild-type cells the 680 nm shoulder increased upon trap closure, but not the 660 nm peak (Figure 8 shows the wild type). As direct excitation of allophycocyanin at 650 nm did not generate the 3.3 ns component, we assign this longest lived decay to uncoupled phycocyanin. The 1.3 ns component observed for excitation of allophycocyanin is clearly a mixture of a component associated with closed PSII reaction centers and a long-lived allophycocyanin decay component. The 1.3 ns allophycocyanin decay component made a much more significant contribution to the overall decay at 650 nm than did the 3.3 ns phycocyanin component at 407 nm. Although both of these components were higher in the mutant than in the wild type, the 1.3 ns component will have contributed more significantly to the increased phycobilin emission observed in the steady-state emission spectra of the mutant. However, the most dramatic difference between mutant and wild type was for the 1 ns PSII component observed at 407 nm excitation whose yield was three times higher in the mutant than the wild type. This suggests that a significant number of PSII reaction centers were closed in the mutant cells at F_o.

DISCUSSION

Previous work with a *Synechocystis* sp. PCC 6803 *psbU* deletion mutant indicated that the PsbU protein affected PSII electron transport by moderating the S-state transitions and stabilizing the S_2 state (*18*, *37*). The *psbU* deletion mutant was also shown to have a reduced rate of oxygen evolution (*17*, *18*). These results are consistent with the lumenal side location of the PsbU protein and its role in stabilizing the OEC. Our picosecond fluorescence decay data confirm an inhibition of electron transport capacity of PSII in the ΔPsbU mutant and show increases in the contribution of fluorescence decay components associated with closed PSII centers in dark-adapted ΔPsbU cells. Specifically, the presence of the 1 ns PSII-associated component at F_o clearly indicates that a significant number of PSII centers remain closed in the mutant in the dark and are thus unavailable for photochemistry and will not contribute to oxygen evolution. The lack of PsbU thus affects the efficiency of PSII photochemistry.

In addition, our results also indicate an increase in the numbers of partially excitonically decoupled PBS in the ΔPsbU strain. This result was unexpected as the PBS and PsbU are located on opposite sides of the thylakoid membrane. Room temperature PAM and fluorescence emission spectroscopy indicate a significant increase in phycobilin fluorescence in cells without PsbU. The 77 K fluorescence emission spectra localize this to allophycocyanin and the terminal phycobilin emitters. This result was confirmed by time-resolved fluorescence decay spectroscopy which showed a large increase in the yield of a 1.3 ns, allophycocyanin-associated, decay component in the mutant cells. This component likely reflects allophycocyanin that is uncoupled from the terminal phycobilin emitters in the PBS.

The mutant cells were also characterized by an increase in a 300 ps fluorescence decay component at F_o whose origin

is complex. This component increased in amplitude upon PSII trap closure but also showed significant contributions by phycobilin core components. The 300 ps component we observed was likely a mixture of two previously observed fluorescence decay components, one associated with closed PSII centers (500 ps) and the other believed to arise from the terminal phycobilin emitter (200 ps) (*36*). The increase in the 300 ps component upon trap closure and in the ΔPsbU mutant at F_o is consistent with the previously observed increase in contribution of the 500 ps PSII component upon trap closure in intact cyanobacteria. This interpretation is supported by the increased yield of the 1 ns decay component, indicative of closed PSII reaction centers, observed in the mutant cells at F_o. Another possible interpretation, especially for 650 nm excitation, is that this component could reflect decay from phycobilin core components including the terminal phycobilin emitters. A 200 ps component associated with the terminal phycobilin emitters had previously been observed in intact cyanobacteria (*36*). In that study the lifetime was attributed to relatively inefficient energy transfer from the terminal emitter to PSII Chl *a*. In a separate study (*38*), a 500 ps component was attributed to the terminal phycobilin emitters in a PSII-less mutant of *Synechocystis* sp. PCC 6803. That decay was much faster than the 1.5 ns decay associated with emission from the terminal phycobilin emitters in isolated PBS and was attributed to quenching associated with PBS binding to the thylakoid membrane. The increased amplitude of the 300 ps component observed in the ΔPsbU cells in our study may thus reflect an increase in the number of PBS energetically uncoupled from PSII, but still attached to the thylakoid membrane. This interpretation would be consistent with the transient coupling model of PBS and PSII interaction supported by FRAP data (*10*, *13*) assuming that the terminal emitter decay in the coupled PBS/PSII complex was much shorter than the 300 ps decay component and not observed in our measurements.

Any assessment of the effect that the removal of PsbU has on the energetic coupling of the PBS to PSII is hampered by the lack of consensus on the mechanism of coupling (*8*, *13*). There is a PB loop of the L(CM) domain or hydrophobic linker peptide chain that has been suspected to be involved in either PSII or membrane binding and energy transfer (*8*). Thus it is plausible to infer a disruption in the binding of this linker peptide to PSII and/or the thylakoid membrane when PSII centers do not contain PsbU. However, previous work has shown that the PBS still assembles and functions comparably with wild type in mutants that have the PB loop deleted from the L(CM) domain (*12*). A "native affinity" has also been demonstrated in vitro, whereby isolated PSII complexes and PBS were found to energetically couple without a thylakoid membrane or PB loop on the PBS (*11*). The native affinity between PSII and the PBS may provide the most likely factor in PSII/PBS energy coupling that is being affected by the removal of PsbU. Energetic coupling from the PBS to PSII and PSI is likely mediated through the phycobilin terminal emitters, which are three long-wavelength allophycocyanin pigments associated with ApcD, ApcE, and ApcF. It is uncertain how these long-wavelength emitters couple energetically to the Chl of PSII and PSI, although a number of proposals have been put forward (*8*, *39*, *40*). It is clear, however, that the energetic coupling of the PBS will be highly dependent on the distance between, and relative orientations of, the terminal PBS emitters and Chl molecules in the PSII core. We propose that the absence of PsbU on the lumenal side of the PSII core may affect a small overall change in PSII core structure which is correlated with a subtle change in the stromal exposed surface of PSII. Modification of the donor side of PSII has previously been shown to influence the acceptor side (*41*). A small change in the shape of the stromal exposed surface of PSII could significantly affect the interaction of the PSII core with the PBS and thus disrupt energy transfer from one or more of these pigments to the core Chl of PSII. We have demonstrated that the PsbU protein influences diverse processes in PSII. Electron transport activity is limited in the absence of PsbU as a proportion of PSII centers remain closed in dark-adapted cells. In addition, the absence of PsbU impairs energy transfer from the PBS to PSII. PsbU thus serves roles in stabilizing both electron transport and energy transfer in the PBS/PSII assembly in *Synechocystis* sp. PCC 6803.

REFERENCES

1. Barber, J. (2003) Photosystem II: the engine of life, *Q. Rev. Biophys. 36*, 71−89.
2. Ferreira, K. N., Iverson, T. M., Maghlaoui, K., Barber, J., and Iwata, S. (2004) Architecture of the photosynthetic oxygen-evolving center, *Science 303*, 1831−1838.
3. Bricker, T. M., and Frankel, L. K. (2002) The structure and function of CP47 and CP43 in photosystem II, *Photosynth. Res. 72*, 131−146.
4. Eaton-Rye, J. J., and Putnam-Evans, C. (2005) The CP47 and CP43 core antenna components, in *Photosystem II: The Water/Plastoquinone Oxido-Reductase of Photosynthesis* (Wydrzynski, T., and Satoh, K., Eds.) Springer, Dordrecht (in press).
5. Ananyev, G. M., Zaltsman, L., Vasko, C., and Dismukes, G. C. (2001) The inorganic biochemistry of photosynthetic oxygen evolution/water oxidation, *Biochim. Biophys. Acta 1503*, 52−68.
6. Kok, B., Forbush, B., and McGloin, M. (1970) Cooperation of charges in photosynthetic O_2 evolution−I. A linear four-step mechanism, *Photobiochem. Photobiol. 11*, 457−475.
7. Debus, R. J. (2000) The polypeptides of photosystem II and their influences on mangano-tyrosyl based oxygen evolution, in *Metal Ions in Biological Systems* (Sigel, A., and Sigel, H., Eds.) Vol. 37, pp 657−711, Marcel Dekker, New York.
8. McConnell, M. D., Koop, R., Vasil'ev, S., and Bruce, D. (2002) Regulation of the distribution of chlorophyll and phycobilin-absorbed excitation energy in cyanobacteria. A structural-based model for the light state transition, *Plant Physiol. 130*, 1201−1212.
9. Bryant, D. A. (1991) Cyanobacterial phycobilisomes: Progress toward complete structural and functional analysis via molecular genetics, in *Cell Culture and Somatic Cell Genetics of Plants, Vol. 7B: The Photosynthetic Apparatus: Molecular Biology and Operation* (Bogorad, L., and Vasil, I. L., Eds.) pp 257−300, Academic Press, San Diego.
10. Mullineaux, C. W., Tobin, M. J., and Jones, G. R. (1997) Mobility of photosynthetic complexes in thylakoid membranes, *Nature 390*, 421−424.
11. Kirilovsky, D., and Ohad, I. (1986) Functional assembly *in vitro* of phycobilisomes with isolated photosystem II particles of eukaryotic chloroplasts, *J. Biol. Chem. 261*, 12317−12323.
12. Ajlani, G., and Vernotte, C. (1998) Deletion of the PB-loop in the L(CM) subunit does not affect phycobilisome assembly or energy transfer functions in the cyanobacterium *Synechocytsis* sp. PCC6714, *Eur. J. Biochem. 257*, 154−159.
13. Sarcina, M., Tobin, M. J., and Mullineaux, C. W. (2001) Diffusion of phycobilisomes on the thylakoid membranes of the cyanobacterium *Synechococcus* 7942, *J. Biol. Chem. 276*, 46830−46834.
14. Ashby, M. K., and Mullineaux, C. W. (1999) The role of ApcD and ApcF in energy transfer from phycobilisomes to PS I and PS II in a cyanobacterium, *Photosynth. Res. 61*, 169−179.
15. Nishiyama, Y., Los, D. A., Hayashi, H., and Murata, N. (1997) Thermal protection of the oxygen-evolving machinery by PsbU,

an extrinsic protein of photosystem II, in *Synechococcus* species PCC 7002, *Plant Physiol. 115*, 1473−1480.
16. Nishiyama, Y., Los, D. A., and Murata, N. (1999) PsbU, a protein associated with photosystem II, is required for the acquisition of cellular thermotolerance in *Synechococcus* species PCC 7002, *Plant Physiol. 120*, 301−308.
17. Kimura, A., Eaton-Rye, J. J., Morita, E. H., Nishiyama, Y., and Hayashi, H. (2002) Protection of the oxygen-evolving machinery by the extrinsic proteins of photosystem II is essential for development of cellular thermotolerance in *Synechocystis* sp. PCC 6803, *Plant Cell Physiol. 43*, 932−938.
18. Shen, J.-R., Ikeuchi, M., and Inoue, Y. (1997) Analysis of the *psbU* gene encoding the 12-kDa extrinsic protein of photosystem II and studies on its role by deletion mutagenesis in *Synechocystis* sp. PCC 6803, *J. Biol. Chem. 272*, 17821−17826.
19. Summerfield, T. C., Shand, J. A., Bentley, F. K., and Eaton-Rye, J. J. (2005) PsbQ (Sll1638) in *Synechocystis* sp. PCC 6803 is required for photosystem II activity in specific mutants and in nutrient-limiting conditions, *Biochemistry 44*, 805−815.
20. Shen, J.-R., and Inoue, Y. (1993) Binding and functional properties of two new extrinsic components, cytochrome *c*-550 and a 12 kDa protein, in cyanobacterial photosystem II, *Biochemistry 32*, 1825−1832.
21. Eaton-Rye, J. J., Shand, J. A., and Nicoll, W. (2003) pH-dependent photoautotrophic growth of specific photosystem II mutants lacking lumenal extrinsic polypeptides in *Synechocystis* PCC 6803, *FEBS Lett. 543*, 148−153.
22. Clarke, S. M., and Eaton-Rye, J. J. (1999) Mutation of Phe-363 in the photosystem II protein CP47 impairs photoautotrophic growth, alters the chloride requirement, and prevents photosynthesis in the absence of either PSII-O or PSII-V in *Synechocystis* sp. PCC 6803, *Biochemistry 38*, 2707−2715.
23. Eaton-Rye, J. J. (2004) The construction of gene knockouts in the cyanobacterium *Synechocystis* sp. PCC 6803, in *Methods in Molecular Biology, Vol. 274: Photosynthesis Research Protocols* (Carpentier, R., Ed.) pp 309−324, Humana Press, Totowa, NJ.
24. Williams, J. G. K. (1988) Construction of specific mutations in the photosystem II photosynthetic reaction center by genetic engineering methods in the cyanobacterium *Synechocystis* 6803, *Methods Enzymol. 167*, 766−778.
25. Boliver, F. (1978) Contruction and characterization of new cloning vehicles, III. Derivatives of plasmid pBR322 carrying unique *Eco*RI sites for selection of *Eco*RI-generated recombinant DNA molecules, *Gene 4*, 121−126.
26. Prentki, P., Karch, F., Iida, S., and Meyer, J. (1981) The plasmid cloning vector pBR325 contains a 482 base-pair-long inverted duplication, *Gene 14*, 289−299.
27. Rouag, D., and Dominy, P. (1994) State adaptations in the cyanobacterium *Synechococcus* 6301 (PCC)—Dependence on light intensity or spectral composition, *Photosynth. Res. 40*, 107−117.
28. Schreiber, U., Hormann, H., Neubauer, C., and Klughammer, C. (1995) Assessment of photosystem II photochemical quantum yield by chlorophyll quenching analysis, *Aust. J. Plant Physiol. 22*, 209−220.
29. Salehian, O., and Bruce, D. (1992) Distribution of excitation energy in photosynthesis: quantification of fluorescence yields from intact cyanobacteria, *J. Lumin. 51*, 91−98.
30. Vasil'ev, S., Wiebe, S., and Bruce, D. (1998) Non-photochemical quenching of chlorophyll fluorescence in photosynthesis. 5-hydroxy-1,4-naphthoquinone in spinach thylakoids as a model for antenna based quenching mechanisms, *Biochim. Biophys. Acta 1363*, 147−156.
31. Vasil'ev, S., and Bruce, D. (1998) Nonphotochemical quenching of excitation energy in photosystem II. A picoscond time-resolved study of the low yield of chlorophyll *a* fluorescence induced by single-turnover flash in isolated spinach thylakoids, *Biochemistry 37*, 11046−11054.
32. Vasil'ev S., and Bruce, D. (2000) Picosecond time-resolved fluorescence studies on excitation energy transfer in a histidine 117 mutant of the D2 protein of photosystem II in *Synechocystis* 6803, *Biochemistry 39*, 14211−14218.
33. MacKinney, G. (1941) Absorption of light by chlorophyll solutions, *J. Biol. Chem. 140*, 315−322.
34. Myers, J., Graham, J.-R., and Wang, R. T. (1980) Light-harvesting in *Anacystis nidulans* studied in pigment mutants, *Plant Physiol. 66*, 1144−1149.
35. Mullineaux, C. W., and Holzwarth, A. R. (1993) Effect of photosystem II reaction centre closure on fluorescence decay kinetics in a cyanobacterium, *Biochim. Biophys. Acta 1183*, 345−351.
36. Mullineaux, C. W., and Holzwarth, A. R. (1991) Kinetics of excitation energy transfer in the cyanobacterial phycobiisome-Photosystem II complex, *Biochim. Biophys. Acta 1098*, 68−78.
37. Shen, J.-R., Qian, M., Inoue, Y., and Burnap, R. L. (1998) Functional characterization of *Synechocystis* sp. PCC 6803 Δ*psb*U and Δ*psb*V mutants reveals important roles of cytochrome *c*-550 in cyanobacterial oxygen evolution, *Biochemistry 37*, 1551−1558.
38. Bittersman, E., and Vermaas, W. (1991) Fluorescence lifetime studies of cyanobacterial photosystem II mutant, *Biochim. Biophys. Acta 1098*, 105−116.
39. Bald, D., Kruip, J., and Rögner, M. (1996) Supramolecular architecture of cyanobacterial thylakoid membranes: How is the phycobilisome connected with the photosystems?, *Photosynth. Res. 49*, 103−118.
40. Barber, J., Norris, E. P., and da Fonseca, C. A. (2003) Interaction of the allophycocyanin core complex with photosytem II, *Photochem. Photobiol. Sci. 2*, 536−541.
41. Johnson, G. N., Rutherford, A. W., and Krieger, A. (1995) A change in the midpoint potential of the quinone Q(A) in photosystem II associated with photoinactivation of oxygen evolution, *Biochim. Biophys. Acta* 1229, 202−207.

BI051137A